Macromolecules

Article

pubs.acs.org/Macromolecules

Synthesis of Nanoparticle Copolymer Brushes via Surface-Initiated *se*ATRP

Paweł Chmielarz,[†,‡] Jiajun Yan,[‡] Pawel Krys,[‡] Yi Wang,[‡] Zongyu Wang,[‡] Michael R. Bockstaller,[§] and Krzysztof Matyjaszewski*[,‡]

[†]Department of Physical Chemistry, Faculty of Chemistry, Rzeszow University of Technology, Al. Powstańców Warszawy 6, 35-959 Rzeszow, Poland

[‡]Department of Chemistry and [§]Department of Materials Science and Engineering, Carnegie Mellon University, Pittsburgh, Pennsylvania 15213, United States

Supporting Information

ABSTRACT: Synthesis of densely grafted (co)polymer brushes, including poly(*tert*-butyl acrylate) (P*t*BA), poly(*tert*-butyl acrylate)-*b*-poly(styrene) (P*t*BA-*b*-PS), and poly(*tert*-butyl acrylate)-*b*-poly(butyl acrylate) (P*t*BA-*b*-PBA), from 15.8 nm silica nanoparticles (NPs) via a surface-initiated simplified electrochemically mediated atom transfer radical polymerization (SI-*se*ATRP) under constant potential electrolysis conditions is reported for the first time. The rate of polymerization was enhanced by applying more negative potentials, which resulted in an increase in grafting density, up to 0.93 nm^{-2}. Furthermore, temporal control over the polymerization was achieved by adjustment of the applied potential. The polymers showed narrow molecular weight distributions ($Đ$ = 1.20−1.32), and polymer-grafted nanoparticles had excellent size uniformity. Dispersions in suitable solvents were stable without any nanoparticle aggregation. Microstructures observed in thin films of densely block copolymer tethered silica NPs suggested that the structure formation process is strongly influenced by the conformation of tethered chains. Hence, microstructure formation in thin films of block copolymer brush particles in which the first block is in the "stretched brush regime" was determined primarily by surface interactions rather than microphase separation.

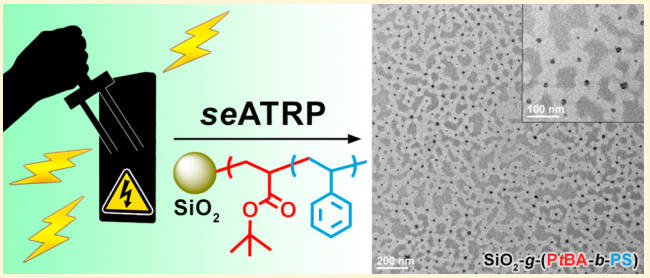

INTRODUCTION

Various silica nanoparticles (NPs) are commercially available and are used in industrial applications, such as catalysis, pigments, electronics, thin film substrates, electric and thermal insulators, humidity sensors, pharmacy, and biomedical approaches, such as drug delivery, bioimaging, sensing, and therapeutics.[1−8] Tethering polymeric chains to the surface of nanosized inorganic particles has emerged as a powerful approach to stabilize NPs dispersions and "engineer" the physicochemical properties of particles but also as a route toward the synthesis of nanocomposite materials with new functionalities.[9−15] Preparation of stable inorganic−organic hybrid materials involves covalent binding of the polymer chains to the nanoparticles. This can be achieved e.g. via a *grafting-onto* approach, where polymer chains containing end-functional groups are synthesized and subsequently attached to the surface of the nanoparticles modified with complementary functional groups. This method is typically limited by the slow diffusion of polymer chains to the surface of the substrate and by the steric hindrance of the tethering sites arising from formation of random coils by the attached polymer chains.[10,16] Another technique, *grafting-through*, utilizes tethering units of a polymerizable monomer to the surface of the nanoparticle. Subsequently, the covalently attached monomer is copolymerized with a low molecular weight monomer present in the contacting solution, yielding tethered polymers.[15] This method is less common, since it typically results in lower grafting densities. Finally, the *grafting-from* method involves two steps: binding low molecular weight initiating groups to the surface of the particle and subsequent formation of polymers.[16] This is commonly achieved via a reversible-deactivation radical polymerization (RDRP) methods,[11,15,17] although anionic polymerization,[18] ring-opening metathesis polymerization (ROMP),[19] or conventional radical polymerization[20,21] can also be used. RDRP allows for simultaneous growth of all chains affording high grafting densities and good control over the physicochemical properties of polymer-tethered particles.[22,23]

RDRP methods most commonly used for *grafting-from* include reversible addition−fragmentation chain transfer (RAFT) polymerization,[24] nitroxide-mediated polymerization (NMP),[25] and atom transfer radical polymerization (ATRP).[11,15,26] Surface-initiated ATRP (SI-ATRP) is one of the most established approaches to form hybrid particles.[10,11,15,17] It provides excellent control over architecture and wide range of accessible chemistries and compositions of

Received: February 7, 2017
Revised: April 27, 2017
Published: May 17, 2017

DOI: 10.1021/acs.macromol.7b00280
Macromolecules 2017, 50, 4151−4159

Scheme 1. Synthesis of P*t*BA-*b*-PS and P*t*BA-*b*-PBA Brushes from Silica Nanoparticles by *se*ATRP

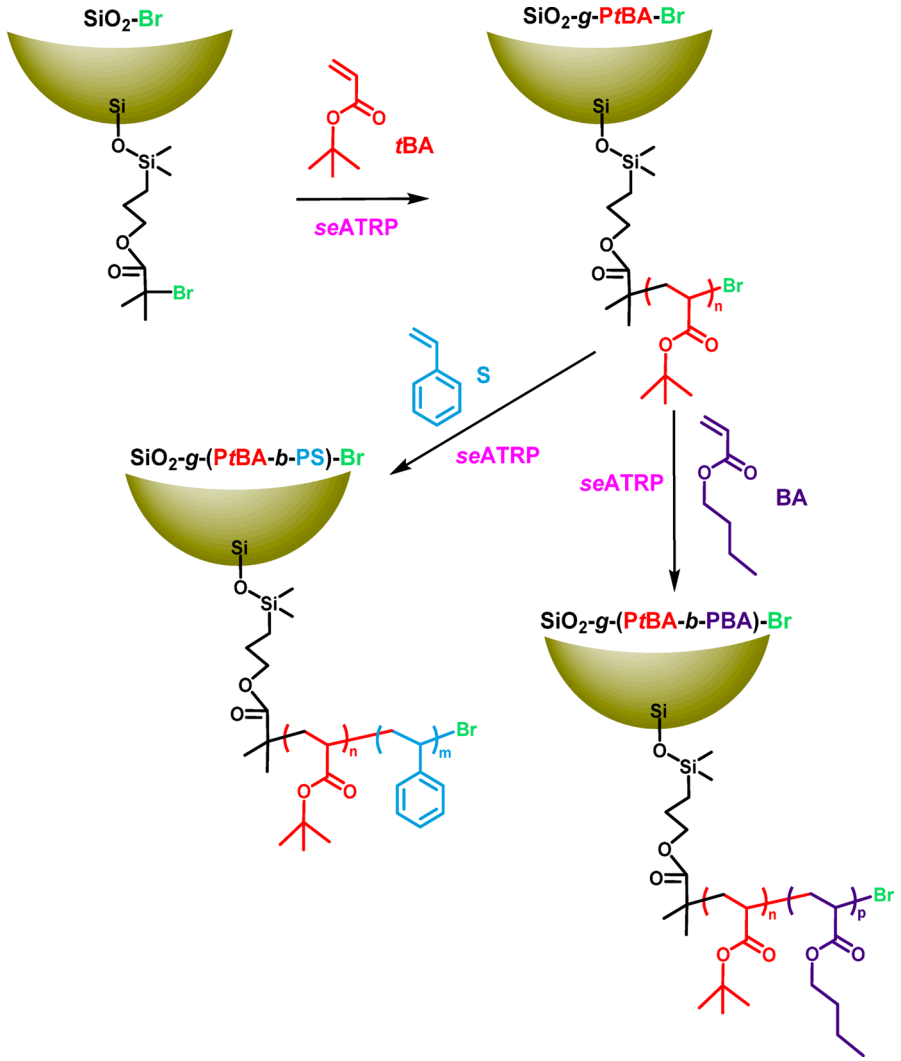

the grafted polymer chains.[11,15,17,27] The hybrid nanoparticle radius can be adjusted via fine-tuning of the grafting density (σ) and degree of polymerization (N) of the tethered chains. SI-ATRP allows one to synthesize well-defined polymer brushes with high grafting densities.[10,11,15,17,22,23,28,29] A wide variety of organic−inorganic hybrid materials, including matrix-free nanocomposites,[26,30,31] compatibilizing fillers,[32] functional additives,[33−35] responsive particles,[36,37] functional surfaces,[38,39] and membranes,[40−43] were successfully prepared via SI-ATRP in the past decade.

Recently, several ATRP techniques utilizing low ppm of catalyst complex have emerged that possess broad capabilities in preparation of polymeric materials.[44,45] This includes activators regenerated by electron transfer (ARGET) ATRP,[46−48] supplemental activator and reducing agent (SARA) ATRP,[49−51] initiators for continuous activator regeneration (ICAR) ATRP,[52,53] photochemically mediated ATRP (photoATRP),[54,55] electrochemically mediated ATRP (*e*ATRP),[56−58] and metal-free ATRP.[59,60] Most of these ATRP techniques were successfully applied to grafting polymer brushes from a range of surfaces of different shapes and compositions.[30,61−67] The opportunity to harness the high level of structural and compositional control that is facilitated by ATRP at reduced Cu concentrations offers intriguing possibilities for the synthesis of hybrid materials. This is because the presence of even small amounts of Cu impurities could be detrimental to the physical properties of hybrid materials (such as optical transparency, dielectric properties, or photothermal stability) which are fundamental to their application in advanced material technologies.

*e*ATRP is of particular interest to the synthesis of functional materials because it does not require the addition of reducing agents (since electrons in this case are provided by an external source). Parameters such as the applied current, applied potential, and total charge passed can be defined in *e*ATRP to allow selection of the desired concentration of redox-active catalytic species, therefore enhancing the level of control during polymerization.[56] *e*ATRP can be even stopped and (re)initiated on demand by modulating the applied potential, offering convenient temporal control over the polymerization.[56,68] Moreover, the procedure is tolerant to small amounts of oxygen and allows a new approach to catalyst removal or recycling via electrodeposition.[58] *e*ATRP has shown versatility in synthesizing wide range of well-defined polymer architectures,[56,58] although some limitations remain, especially associated with the reaction setup. Conventional *e*ATRP requires a three-electrode system composed of a working (WE), a counter (CE), and a reference electrode (RE),

DOI: 10.1021/acs.macromol.7b00280
Macromolecules 2017, 50, 4151−4159

Table 1. Summary of Homopolymer and Block Copolymer Brushes Grafted from Silica NPs[a]

	entry	monomer	$[M]_0/[I]_0/[Cu^{II}Br_2]_0/[TPMA]_0$	E_{app} [b]	k_p^{app} [c] (h^{-1})	$M_{n,th}$ [d] ($\times 10^3$)	$M_{n,app}$ [e] ($\times 10^3$)	$Đ$ [e]	$d_{Z\text{-}ave}$ [f] (nm)	σ [g] (nm^{-2})
homopolymer brushes	1	*t*BA	1050/1[h]/0.105/0.21		0.239	51.2	49.8	1.18	126 ± 1	0.92
	2	*t*BA	1050/1[h]/0.105/0.21	E_{pc} − 120 mV	0.348	58.7	64.5	1.29	147 ± 1	0.93
	3	*t*BA	1050/1[h]/0.105/0.21	E_{pc} − 80 mV	0.286	54.9	60.3	1.21	137 ± 1	0.89
	4	*t*BA	1050/1[h]/0.105/0.21	E_{pc} − 40 mV	0.236	48.5	57.4	1.32	135 ± 1	0.88
	5	*t*BA	1050/1[h]/0.105/0.21	E_{pc}	0.177	38.6	36.0	1.32	86 ± 1	0.71
copolymer brushes	6	S	4000/1[I]/0.4/0.8	E_{pc} − 80 mV	0.014	92.9	86.5	1.20	155 ± 1	0.88
	7	BA	4000/1[I]/0.4/0.8	E_{pc} − 80 mV	0.023	108.0	98.1	1.21	195 ± 1	0.70

[a]General reaction conditions: T = 55 °C; V_{tot} = 28.2 mL (except entry 1: V_{tot} = 10 mL); t = 1.73 h (except entry 6: t = 5 h, entry 7: t = 4 h); $[tBA]_0$ = 3.4 M (except entry 6: $[S]_0$ = 4.3 M and entry 7: $[BA]_0$ = 3.5 M); [I]: $[SiO_2\text{-Br}, \approx 1\ Br/nm^2]_0$ = 3.23 mM (except entry 6: $[SiO_2\text{-}g\text{-}PtBA\text{-}Br]_0$ = 1.08 M and entry 7: $[SiO_2\text{-}g\text{-}PtBA\text{-}Br]_0$ = 0.87 M); [TBAP] = 0.2 M (except entry 1: [TBAP] = 0.0 M). SARA ATRP (Cu^0 wire (l = 1 cm, d = 1 mm, S/V = 0.033 cm^{-1})): entry 1; *se*ATRP under constant potential electrolysis (WE = Pt mesh, CE = Al wire (l = 10 cm, d = 1 mm), RE = Ag/AgI/I^-): entries 2−7. [b]Applied potential (E_{app}) was selected based on cyclic voltammetry (CV) analysis of catalyst complex (Figure 1a, Figures S3a and S4a; ν = 100 mV/s). [c]Monomer conversion was determined by ^{1}H NMR.[72] [d]$M_{n,th} = ([M]_0/[I]_0) \times \text{conversion} \times M_{monomer} + M_{initiator}$. [e]Apparent M_n and $Đ$ were determined from polymer chains untethered from NPs by HF etching using THF SEC with PS standards. [f]Particle size ($d_{Z\text{-}ave}$) was measured by DLS. [g]Grafting density (σ) was calculated from TGA inorganic fraction and eq S1. See Table S1 for details.[64] [h]I = SiO_2-Br (for entries 1−5). [I]I = SiO_2-*g*-P*t*BA-Br indicated as entry 3 in Table 1 (for entries 6 and 7).

resulting in a somewhat complex experimental setup. More recently, a simplified electrochemically mediated ATRP (*se*ATRP) procedure was developed. This procedure does not require the separation of cathodic and anodic compartments in the *e*ATRP reaction system and utilizes a sacrificial counter electrode, thereby significantly simplifying the reaction system.[57,58,69−75] One of the potential advantages of applying *se*ATRP to particle systems is the possibility to produce Cu-free hybrid materials for optical applications. Here we present for the first time grafting well-defined poly(*tert*-butyl acrylate) (P*t*BA), poly(*tert*-butyl acrylate)-*b*-poly(styrene) (P*t*BA-*b*-PS), and poly(*tert*-butyl acrylate)-*b*-poly(butyl acrylate) (P*t*BA-*b*-PBA) brushes from the surfaces of 15.8 nm silica nanoparticles via *se*ATRP (Scheme 1). The effect of applied potential on the polymerization behavior was examined in order to optimize preparation of (co)polymer brushes with low dispersity ($Đ = M_w/M_n$).

RESULTS AND DISCUSSION

Silica NPs with average diameter $\langle d \rangle$ = 15.8 nm were modified by tethering 3-(chlorodimethylsilyl)propyl 2-bromo-2-methyl-propionate initiators to their surface, as described in the literature.[76] The accessible initiator densities of the functionalized particles are typically ≈1 nm^{-2}; however, grafting densities of polymers are usually smaller.[17,23,26,30,76−80] High targeted degrees of polymerization (1050 for homopolymer brushes and 4000 for block copolymer brushes) were selected to provide a sufficiently dilute reaction medium in order to avoid interparticle cross-linking.[11] The *se*ATRP procedure was used for the first time to graft well-defined (co)polymers composed of P*t*BA, P*t*BA-*b*-PS, or P*t*BA-*b*-PBA blocks from silica NPs (Table 1; additional experimental data in the Supporting Information). After the polymerizations were completed, silica cores were etched with HF to provide untethered polymer chains for size-exclusion chromatography (SEC) analysis. In all cases the experimental molecular weight (MW) correlated well with theoretical values and SEC traces (Figure S2) showed well-defined, monomodal polymers with narrow molecular weight distributions (MWDs) ($Đ \leq 1.32$). Purified final products obtained by precipitation in methanol/water mixtures were studied by thermogravimetric analysis (TGA) to determine the fraction of the inorganic content and polymer graft densities (σ). The obtained hybrid materials were also characterized with dynamic light scattering (DLS) and transmission electron microscopy (TEM).

Synthesis of P*t*BA Brushes from Silica NPs by SARA ATRP. Homopolymerization of *t*BA was also conducted via SARA ATRP (Table 1, entry 1) as reference for the electrochemically mediated polymerizations. An induction period was observed, which can be attributed to the necessity to reduce a fraction of the added Cu^{II}/L complex to a sufficient amount of Cu^{I}/L activator (Figure S1a). Afterward, a linear first-order kinetic plot was obtained. The MW of polymers detached from the particles correlated well with theoretical expectation and MWDs remained narrow (Figure S1b). Brushes with a grafting density of ≈0.92 nm^{-2} were obtained, which is comparable with those prepared by *se*ATRP (Table 1, entry 1 vs entries 2−5). SARA ATRP provides a viable route for synthesis of hybrid nanoparticles. However, it has a drawback of gradually introducing additional soluble Cu species into the reaction mixture via supplemental activation of alkyl halides by Cu^0 and comproportionation of Cu^{II} with Cu^0. It was reported that in aqueous SARA ATRP of oligo(ethylene oxide) methyl ether acrylate (M_n = 480) the amount of soluble Cu complexes gradually increased from initially added 100 ppm up to ≈600 ppm.[81] Such an increase might require a more burdensome and costly purification of the desired hybrid material. In contrast, the total amount of soluble Cu species in *se*ATRP is constant and equivalent to the quantity initially introduced into the reaction medium.

Influence of the Applied Potential on Silica NPs Grafting Density. The choice of a suitable applied potential (E_{app}) is crucial when using controlled potential preparative electrolysis.[58] The effect of the E_{app} (E_{pc} − 120 mV, E_{pc} − 80 mV, E_{pc} − 40 mV, and E_{pc}) on the polymerization of *t*BA was investigated (Figure 1a). Similar to our previous studies[58,70−72] faster rates of reduction provided faster polymerizations (Table 1, entries 2−5, and Figure S3b,c). This was caused by the faster regeneration of the activator and resulting higher concentration of the radical species ($[P_n^\bullet]$).[58,82,83] As the rate of polymerization is proportional to $[P_n^\bullet]$ and to the square root of [X−Cu^{II}/L], it can be tuned by the choice of an appropriate E_{app}.[58,82,83]

In all cases a linear relationship was observed between experimental and theoretical MW, and the MWDs remained narrow (Figure 1b and Figure S2a−d), demonstrating good

DOI: 10.1021/acs.macromol.7b00280
Macromolecules 2017, 50, 4151−4159

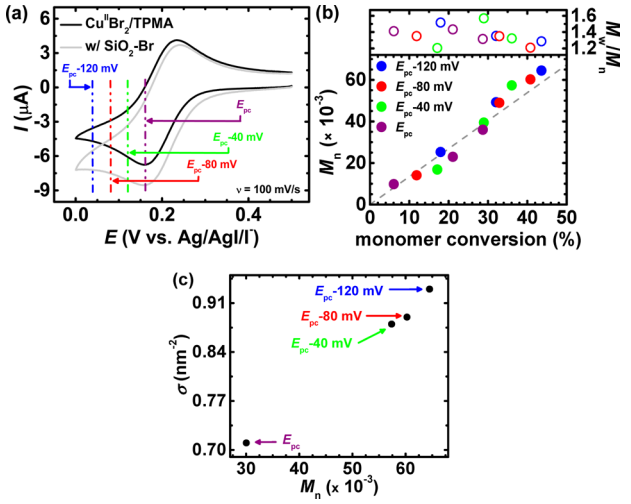

Figure 1. Synthesis of P*t*BA brushes from silica NPs as a function of applied potential. (a) Cyclic voltammetry of $Cu^{II}Br_2$/TPMA with and without initiator (vertical lines indicate E_{app}), (b) M_n and M_w/M_n vs monomer conversion, and (c) grafting density (σ) vs M_n. Reaction conditions: [*t*BA]/[SiO_2-Br]/[$Cu^{II}Br_2$]/[TPMA] = 1050/1/0.105/0.21, $[tBA]_0$ = 3.4 M, T = 55 °C, [TBAP] = 0.2 M, V_{tot} = 28.2 mL. Table 1, entries 2–5.

control over the polymerization. Both the MW of the P*t*BA homopolymer brushes etched from the silica NPs (38 600–58 700) and the grafting density (0.71–0.93 nm^{-2}) of the polymers attached to the NPs correlated well with the applied reduction potential (Figure 1c).

Temporal Control over Polymerization. Application of external stimuli offered an exclusive possibility of temporal control, i.e., the stopping and restarting of the polymerization process by switching the stimuli "off" and "on", respectively.[58,84] Despite multiple on/off cycles, high chain-end functionality was retained without compromising MW and MWD. This was previously demonstrated for *e*ATRP under homogeneous conditions by appropriately adjusting the applied potential.[56,58] A similar effect was obtained by turning the light source on and off in photoATRP.[85] However, due to the use of nanoparticles in the current study, substantial light scattering could interfere or prevent efficient polymerization.[64] Therefore, *e*ATRP offers a unique opportunity to synthesize well-defined hybrid nanoparticles with predefined size. To demonstrate the possibility of temporal control, *se*ATRP was carried out utilizing multiple-step potential electrolysis (Figure 2 and Figure S2g).

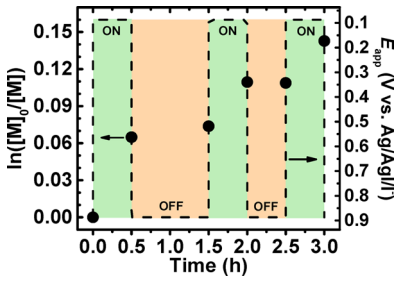

Figure 2. First-order kinetic plot of *se*ATRP with periodically applied different values of potential. Reaction conditions: [*t*BA]/[SiO_2-Br]/[$Cu^{II}Br_2$]/[TPMA] = 1050/1/0.021/0.042, $[tBA]_0$ = 3.4 M in DMF, T = 55 °C, [TBAP] = 0.2 M, V_{tot} = 28.2 mL. ON potential = E_{pc} − 80 mV; OFF potential = E_{pc} + 720 mV.

When negative potential was applied ("ON" = E_{pc} − 80 mV), the reaction proceeded as expected. However, shortly upon applying more positive potential ("OFF" = E_{pc} + 720 mV) the reaction stopped. It was efficiently restarted when the ON potential was reapplied. Such "pausing" of the reaction could be beneficial in preparation of hybrid nanoparticles with predictable molecular weights of the polymer grafts. After analysis, the reaction can easily be restarted, should longer grafts be required.

Chain Extension of SiO_2-*g*-P*t*BA Brushes. The procedure to form diblock brushes was analogous to that of the homopolymer brushes, with the exception that a P*t*BA brush modified silica NPs were used instead of ATRP initiator modified NPs. This new SI-*se*ATRP technique offers some advantages in preparation of block copolymer tethered nanoparticles, e.g., straightforward setup, enhanced control over polymerization rate, high achievable graft densities, and use of low amount of transition metal catalyst. The chain extension from P*t*BA brushes (Table 1, entry 3) with styrene (S) was conducted under constant potential preparative electrolysis conditions (Figure S4). A linear first-order kinetic plot was obtained (Figure 3a), and SEC traces demonstrated

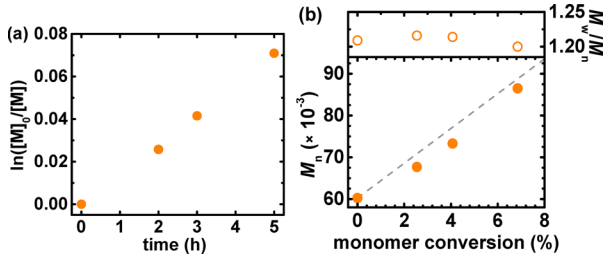

Figure 3. Chain extension of the P*t*BA-functionalized silica nanoparticles with styrene. (a) First-order kinetic plot of monomer conversion vs time and (b) M_n and M_w/M_n vs monomer conversion. Reaction conditions: [S]/[SiO_2-*g*-P*t*BA-Br]/[$Cu^{II}Br_2$]/[TPMA] = 4000/1/0.4/0.8, $[S]_0$ = 4.3 M, T = 55 °C, [TBAP] = 0.2 M, V_{tot} = 28.2 mL. Table 1, entry 6.

narrow MWD of the obtained polymer (Figure 3b and Figure S2e). High grafting density of ≈0.88 nm^{-2} was attained (Table 1, entry 6). Grafting densities of ≈0.63 nm^{-2} were previously reported for PS-tethered SiO_2 particle brush materials prepared by SI-ATRP.[80]

Finally, chain extension of the P*t*BA brushes (Table 1, entry 3) with BA was conducted under constant potential electrolysis conditions (Figure S5). The polymerization was well-controlled with a linear first-order kinetic plot (Figure 4a). P*t*BA-*b*-PBA block copolymers etched from the silica NPs showed good correlation between experimental and theoretical MW and narrow MWD (Figure 4b and Figure S2f). The reaction yielded brushes with a relatively high grafting density of ≈0.71 nm^{-2} that matches previously reported results for homopolymer grafted systems (Table 1, entry 7). For example, silica nanoparticles grafted with homopolymer PBA brushes with graft densities of around 0.80 nm^{-2} were reported.[86]

Material Characterization. The silica hybrid materials were characterized with transmission electron microscopy (TEM), dynamic light scattering (DLS), and differential scanning calorimetry (DSC). Transmission electron microscopy (TEM) was carried out using a JEOL 2000 EX electron microscope operated at 200 kV. TEM images demonstrated successful grafting of P*t*BA from silica nanoparticles and

DOI: 10.1021/acs.macromol.7b00280
Macromolecules 2017, 50, 4151–4159

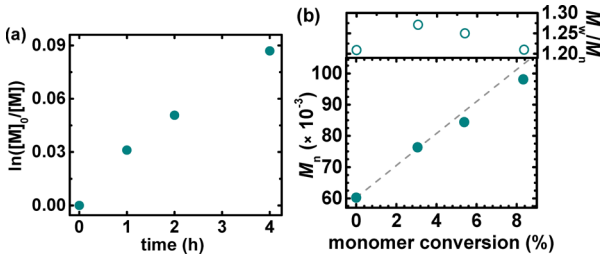

Figure 4. Chain extension of the P*t*BA-functionalized silica nanoparticles with BA. (a) First-order kinetic plot of monomer conversion vs time and (b) M_n and M_w/M_n vs monomer conversion. Reaction conditions: [BA]/[SiO_2-*g*-P*t*BA-Br]/[$Cu^{II}Br_2$]/[TPMA] = 4000/1/0.4/0.8, $[BA]_0$ = 3.5 M, T = 55 °C, [TBAP] = 0.2 M, V_{tot} = 28.2 mL. Table 1, entry 7.

showed no aggregated nanoparticles (Figure 5a, Figures S8a and S9a,c,e,g) as compared to the unmodified silica NPs

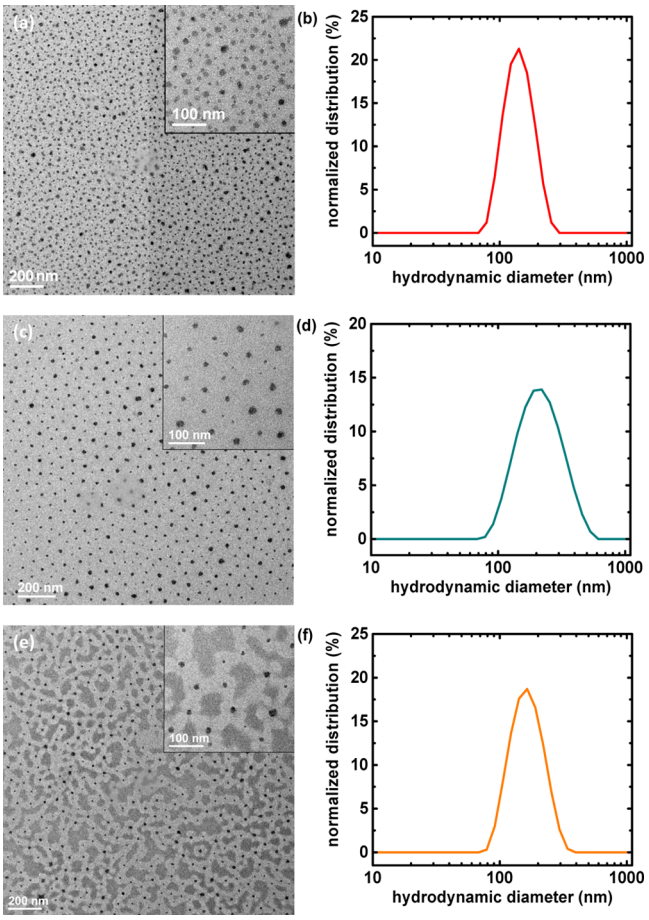

Figure 5. TEM images and DLS hydrodynamic size distributions by intensity (in THF) of (approximately) monolayer films of particle brushes grafted on silica NPs via *se*ATRP: P*t*BA (a, b; Table 1, entry 3), P*t*BA-*b*-PBA (c, d; Table 1, entry 7), and P*t*BA-*b*-PS (e, f; Table 1, entry 6).

(Figure S7). The particle size dispersity was determined by the pristine NP product. Nonetheless, a relatively narrow size distribution of polymer-grafted nanoparticles was observed (Figure 5b, Figures S8b and S9b,d,f,h) which was interpreted as a consequence of the uniform increase of the total particle size upon surface polymerization. Increase of the degree of polymerization of P*t*BA brushes provided a linear increase of the particle size, i.e., $h \sim N$ where h denotes the "brush height" that is equal to one-half of the surface-to-surface distance between neighboring particles (Figure S3e). The same relationship was observed for P*t*BA brushes prepared via *se*ATRP under on/off multiple-step potential electrolysis (Figure S10a–d). This supported the conclusion that the densely grafted polymer brushes were in the concentrated particle brush (CPB) regime.[26,29] This is in agreement with theoretical predictions of the conformation of tethered chain in brush particles. For example, Fukuda and co-workers reported an extended Doud–Cotton model to predict the chain conformation of tethered chains.[23] Based on this model a transition from stretched chain conformations (CPB regime) to random-walk type conformation (semidilute polymer brush, SDPB, regime) is expected at $N_{crit} \approx 10^3$ for σ of 0.8–1.0 nm^{-2} when grafting from 15 nm NPs.[26,87] Based on this estimate, the stretched–coiled transition was expected to occur after chain extension. This agreed well with experimental observations on the dependence of brush height on the degree of polymerization of tethered chains. After chain extension (with either S or BA) excellent particle size uniformity was obtained, and dispersions were stable without indication of aggregation (Figure 5c–f).

Grafting of PBA resulted in an increase of the brush height (Figure 5c), which was in good agreement with the observed increase in hydrodynamic diameter to D_H = 195 ± 1 nm (Figure 5d). Note that electron micrographs of SiO_2-P*t*BA-*b*-PBA particle brush monolayer such as shown in Figure 5c did not reveal insight into the state of microphase separation of the block copolymer ligand. This is attributed to the very similar electron density and reactivity of P*t*BA and PBA segments that prevents contrast formation (or selective staining) of domains. To elucidate the microstructure, the glass transition temperatures were analyzed using DSC. As shown in Figure S11a, DSC analysis of the P*t*BA brush modified silica NPs (Table 1, entry 3) exhibited a single T_g at ca. 44 °C, which is approximately equal to the T_g of the P*t*BA homopolymer.[88] P*t*BA-*b*-PS diblock copolymers attached to silica NPs (Table 1, entry 6) showed two distinct T_g values (Figure S11b) at 46 and 100 °C, corresponding to the T_g values of P*t*BA[88] and PS[30,80,89] blocks, respectively. Also, two T_g values (−16 and 42 °C; Figure S11c,d) were observed in P*t*BA-*b*-PBA diblock copolymers attached to silica NPs (Table 1, entry 7). In this case, however, T_g value of −16 °C was in between the T_g of the PBA and P*t*BA homopolymers (−55 °C[89] and 44 °C,[88] respectively), which suggested partial miscibility of the of the PBA block with the outer part of P*t*BA block. The presence of the second T_g at 42 °C, corresponding to the P*t*BA homopolymer, suggests immiscibility of the most inner part of the P*t*BA chains, which are very densely packed, close to the silica surface.

Analysis of the electron micrograph of the SiO_2-P*t*BA-*b*-PS system (Figure 5e) provides intriguing insight into the morphology of particle brush monolayer structures. We rationalize the microstructure observed in Figure 5e as a consequence of the symmetry-breaking effect of the polymer/air (and to a lesser extent the polymer/substrate) interface. To illustrate the idea, we note that the regular assembly of spherical SiO_2-P*t*BA-*b*-PS brush particles would be expected to result in an "undulated" surface topology that is indicated in the upper image of Figure 6.

DOI: 10.1021/acs.macromol.7b00280
Macromolecules 2017, 50, 4151–4159

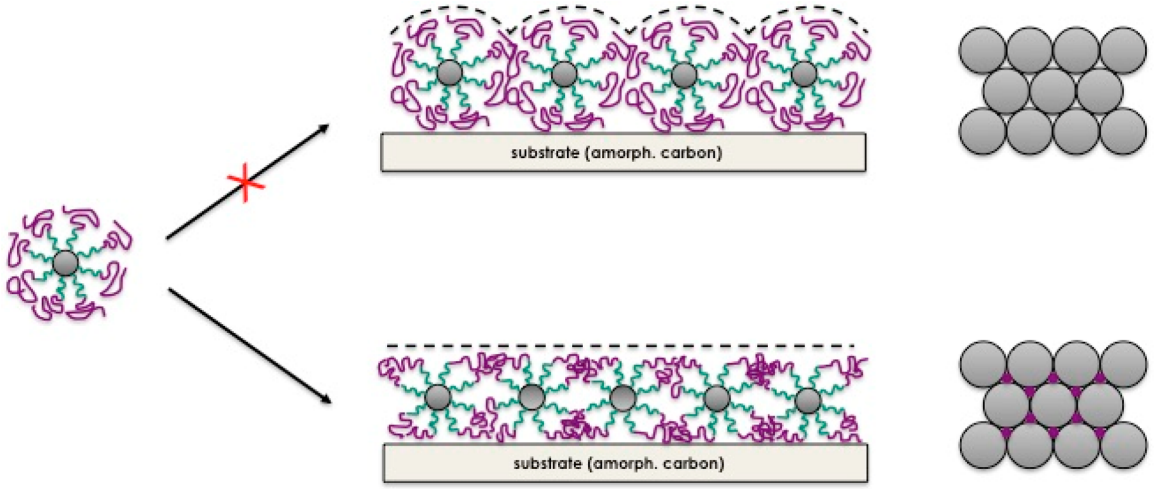

Figure 6. Illustration of the proposed structure formation process resulting in the morphology seen in Figure 5e. Relaxed PS segments (indicated as "purple" block) stretch to fill in the void space in between adjacent brush particles and to minimize the total area of the polymer/air interface (indicated as black dotted line).

This situation is energetically unfavorable since it will create an excess surface area (and hence energy). To reduce the total interface area, the relaxed brush segments are expected to stretch and fill the interstitial space as indicated in the lower panel of Figure 6 (the energy penalty associated with the stretching of chains is considered negligible when compared to the interfacial energy of PS γ_{PS} = 40 mJ/m^2).[90] Since only the "outer" PS block is expected to be in the stretched regime, this causes a "redistribution" of PS chains that causes a characteristic 6-fold contrast pattern in electron micrographs that is approximately observed in Figure 5e. We note that this process bears similarity to the segregation of filler additives to the void spaces in assembly structures formed by brush particles blended with homopolymer or nanoparticle fillers.[88,91] To the best of our knowledge, this is the first example of such phase separation behavior of block copolymers grafted from nanoparticles.

CONCLUSIONS

Well-defined densely grafted (co)polymer brushes were synthesized for the first time via a recently developed surface-initiated simplified electrochemically mediated atom transfer radical polymerization (SI-*se*ATRP) from 15.8 nm silica nanoparticles under constant potential preparative electrolysis conditions. The attractiveness of the presented method stems from the ability to prepare well-defined block copolymer brushes with the desired composition. The controlled/living characteristics of the system allowed for chain extension of the grafted P*t*BA brushes with a second PS or PBA block. Grafting densities up to 0.93 nm^{-2} were obtained. The rate of the polymerizations was enhanced by applying more negative potential values, which also resulted in an increase of grafting densities. Facile temporal control over polymerization was achieved by appropriately varying applied potential. All prepared (co)polymer brushes had narrow MWDs ($Đ$ = 1.20−1.32). Excellent polymer-grafted nanoparticle size uniformity was obtained, and dispersions were stable without indication of any trace of nanoparticles aggregation. Microstructure formation observed in thin films of densely block copolymer tethered silica NPs revealed a strong influence of the conformation of tethered chains. In particular, if the first block is in the "stretched brush regime", then structure formation was determined primarily by surface interactions rather than microphase separation. For the specific case of the densely tethered SiO_2-P*t*BA-*b*-PS system the relaxed outer PS segments stretched to fill in the void space in between adjacent brush particles and to minimize the total area of the polymer/air interface.

ASSOCIATED CONTENT

Supporting Information

The Supporting Information is available free of charge on the ACS Publications website at DOI: 10.1021/acs.macromol.7b00280.

Experimental conditions, table, figures showing DLS results and SEC traces of polymers, kinetic results, CV results, TEM images of functionalized silica NPs (PDF)

AUTHOR INFORMATION

Corresponding Author

*E-mail: km3b@andrew.cmu.edu (K.M.).

ORCID

Paweł Chmielarz: 0000-0002-9101-6264
Jiajun Yan: 0000-0003-3286-3268
Michael R. Bockstaller: 0000-0001-9046-9539
Krzysztof Matyjaszewski: 0000-0003-1960-3402

Notes

The authors declare no competing financial interest.

ACKNOWLEDGMENTS

Financial support from NSF (DMR 1501324, CMMI 1663305) is gratefully acknowledged. P.C. acknowledges Kosciuszko Foundation Fellowship. J.Y. acknowledges the Richard King Mellon Foundation Presidential Fellowship. P.K. acknowledges Dr. Konrad M. Weis Fellowship in Chemistry.

REFERENCES

(1) Rao, K. S.; El-Hami, K.; Kodaki, T.; Matsushige, K.; Makino, K. A Novel Method for Synthesis of Silica Nanoparticles. *J. Colloid Interface Sci.* **2005**, *289* (1), 125−131.

DOI: 10.1021/acs.macromol.7b00280
Macromolecules 2017, 50, 4151−4159

(2) Burns, A.; Ow, H.; Wiesner, U. Fluorescent Core-Shell Silica Nanoparticles: Towards "Lab on a Particle" Architectures for Nanobiotechnology. *Chem. Soc. Rev.* **2006**, *35* (11), 1028−1042.
(3) Slowing, I. I.; Trewyn, B. G.; Giri, S.; Lin, V. S. Y. Mesoporous Silica Nanoparticles for Drug Delivery and Biosensing Applications. *Adv. Funct. Mater.* **2007**, *17* (8), 1225−1236.
(4) Slowing, I. I.; Trewyn, B. G.; Lin, V. S. Y. Mesoporous Silica Nanoparticles for Intracellular Delivery of Membrane-Impermeable Proteins. *J. Am. Chem. Soc.* **2007**, *129* (28), 8845−8849.
(5) Lu, J.; Liong, M.; Zink, J. I.; Tamanoi, F. Mesoporous Silica Nanoparticles as a Delivery System for Hydrophobic Anticancer Drugs. *Small* **2007**, *3* (8), 1341−1346.
(6) Torney, F.; Trewyn, B. G.; Lin, V. S. Y.; Wang, K. Mesoporous Silica Nanoparticles Deliver DNA and Chemicals into Plants. *Nat. Nanotechnol.* **2007**, *2* (5), 295−300.
(7) Li, Z.; Barnes, J. C.; Bosoy, A.; Stoddart, J. F.; Zink, J. I. Mesoporous Silica Nanoparticles in Biomedical Applications. *Chem. Soc. Rev.* **2012**, *41* (7), 2590−2605.
(8) Tang, F.; Li, L.; Chen, D. Mesoporous Silica Nanoparticles: Synthesis, Biocompatibility and Drug Delivery. *Adv. Mater.* **2012**, *24* (12), 1504−1534.
(9) Pyun, J.; Kowalewski, T.; Matyjaszewski, K. Synthesis of Polymer Brushes Using Atom Transfer Radical Polymerization. *Macromol. Rapid Commun.* **2003**, *24* (18), 1043−1059.
(10) Tsujii, Y.; Ohno, K.; Yamamoto, S.; Goto, A.; Fukuda, T. Structure and Properties of High-Density Polymer Brushes Prepared by Surface-Initiated Living Radical Polymerization. *Adv. Polym. Sci.* **2006**, *197*, 1−45.
(11) Hui, C. M.; Pietrasik, J.; Schmitt, M.; Mahoney, C.; Choi, J.; Bockstaller, M. R.; Matyjaszewski, K. Surface-Initiated Polymerization as an Enabling Tool for Multifunctional (Nano-)Engineered Hybrid Materials. *Chem. Mater.* **2014**, *26* (1), 745−762.
(12) Fernandes, N. J.; Koerner, H.; Giannelis, E. P.; Vaia, R. A. Hairy Nanoparticle Assemblies as One-Component Functional Polymer Nano-composites: Opportunities and Challenges. *MRS Commun.* **2013**, *3* (1), 13−29.
(13) Kumar, S. K.; Jouault, N.; Benicewicz, B.; Neely, T. Nanocomposites with Polymer Grafted Nanoparticles. *Macromolecules* **2013**, *46* (9), 3199−3214.
(14) Hilburg, S. L.; Elder, A. N.; Chung, H.; Ferebee, R. L.; Bockstaller, M. R.; Washburn, N. R. A Universal Route Towards Thermoplastic Lignin Composites with Improved Mechanical Properties. *Polymer* **2014**, *55* (4), 995−1003.
(15) Khabibullin, A.; Mastan, E.; Matyjaszewski, K.; Zhu, S. Surface-Initiated Atom Transfer Radical Polymerization. *Adv. Polym. Sci.* **2015**, *270*, 29−76.
(16) Radhakrishnan, B.; Ranjan, R.; Brittain, W. J. Surface Initiated Polymerizations from Silica Nanoparticles. *Soft Matter* **2006**, *2* (5), 386−396.
(17) Barbey, R.; Lavanant, L.; Paripovic, D.; Schüwer, N.; Sugnaux, C.; Tugulu, S.; Klok, H.-A. Polymer Brushes via Surface-Initiated Controlled Radical Polymerization: Synthesis, Characterization, Properties, and Applications. *Chem. Rev.* **2009**, *109* (11), 5437−5527.
(18) Zhou, Q.; Wang, S.; Fan, X.; Advincula, R.; Mays, J. Living Anionic Surface-Initiated Polymerization (LASIP) of a Polymer on Silica Nanoparticles. *Langmuir* **2002**, *18* (8), 3324−3331.
(19) Watson, K. J.; Zhu, J.; Nguyen, S. T.; Mirkin, C. A. Hybrid Nanoparticles with Block Copolymer Shell Structures. *J. Am. Chem. Soc.* **1999**, *121* (2), 462−463.
(20) Prucker, O.; Rühe, J. Synthesis of Poly(styrene) Monolayers Attached to High Surface Area Silica Gels through Self-Assembled Monolayers of Azo Initiators. *Macromolecules* **1998**, *31* (3), 592−601.
(21) Prucker, O.; Rühe, J. Mechanism of Radical Chain Polymerizations Initiated by Azo Compounds Covalently Bound to the Surface of Spherical Particles. *Macromolecules* **1998**, *31* (3), 602−613.
(22) Ohno, K.; Koh, K.; Tsujii, Y.; Fukuda, T. Fabrication of Ordered Arrays of Gold Nanoparticles Coated with High-Density Polymer Brushes. *Angew. Chem., Int. Ed.* **2003**, *42* (24), 2751−2754.
(23) Ohno, K.; Morinaga, T.; Koh, K.; Tsujii, Y.; Fukuda, T. Synthesis of Monodisperse Silica Particles Coated with Well-Defined, High-Density Polymer Brushes by Surface-Initiated Atom Transfer Radical Polymerization. *Macromolecules* **2005**, *38* (6), 2137−2142.
(24) Li, C.; Han, J.; Ryu, C. Y.; Benicewicz, B. C. A Versatile Method To Prepare RAFT Agent Anchored Substrates and the Preparation of PMMA Grafted Nanoparticles. *Macromolecules* **2006**, *39* (9), 3175−3183.
(25) Bartholome, C.; Beyou, E.; Bourgeat-Lami, E.; Chaumont, P.; Zydowicz, N. Nitroxide-Mediated Polymerizations from Silica Nanoparticle Surfaces: "Graft from" Polymerization of Styrene Using a Triethoxysilyl-Terminated Alkoxyamine Initiator. *Macromolecules* **2003**, *36* (21), 7946−7952.
(26) Choi, J.; Hui, C. M.; Pietrasik, J.; Dong, H.; Matyjaszewski, K.; Bockstaller, M. R. Toughening Fragile Matter: Mechanical Properties of Particle Solids Assembled from Polymer-Grafted Hybrid Particles Synthesized. *Soft Matter* **2012**, *8* (15), 4072−4082.
(27) Pyun, J.; Matyjaszewski, K. Synthesis of Nanocomposite Organic/Inorganic Hybrid Materials Using Controlled "Living" Radical Polymerization. *Chem. Mater.* **2001**, *13* (10), 3436−3448.
(28) Yoshikawa, C.; Goto, A.; Tsujii, Y.; Fukuda, T.; Yamamoto, K.; Kishida, A. Fabrication of High-Density Polymer Brush on Polymer Substrate by Surface-Initiated Living Radical Polymerization. *Macromolecules* **2005**, *38* (11), 4604−4610.
(29) Ohno, K.; Morinaga, T.; Takeno, S.; Tsujii, Y.; Fukuda, T. Suspensions of Silica Particles Grafted with Concentrated Polymer Brush: Effects of Graft Chain Length on Brush Layer Thickness and Colloidal Crystallization. *Macromolecules* **2007**, *40* (25), 9143−9150.
(30) Yan, J.; Kristufek, T.; Schmitt, M.; Wang, Z.; Xie, G.; Dang, A.; Hui, C. M.; Pietrasik, J.; Bockstaller, M. R.; Matyjaszewski, K. Matrix-free Particle Brush System with Bimodal Molecular Weight Distribution Prepared by SI-ATRP. *Macromolecules* **2015**, *48* (22), 8208−8218.
(31) Huang, Y.; Huang, X.; Schadler, L. S.; He, J.; Jiang, P. Core@Double-Shell Structured Nanocomposites: A Route to High Dielectric Constant and Low Loss Material. *ACS Appl. Mater. Interfaces* **2016**, *8* (38), 25496−25507.
(32) Dang, A.; Ojha, S.; Hui, C. M.; Mahoney, C.; Matyjaszewski, K.; Bockstaller, M. R. High-Transparency Polymer Nanocomposites Enabled by Polymer-Graft Modification of Particle Fillers. *Langmuir* **2014**, *30* (48), 14434−14442.
(33) Ojha, S.; Dang, A.; Hui, C. M.; Mahoney, C.; Matyjaszewski, K.; Bockstaller, M. R. Strategies for the Synthesis of Thermoplastic Polymer Nanocomposite Materials with High Inorganic Filling Fraction. *Langmuir* **2013**, *29* (28), 8989−8996.
(34) Halim, A.; Fu, Q.; Yong, Q.; Gurr, P. A.; Kentish, S. E.; Qiao, G. G. Soft Polymeric Nanoparticle Additives for Next Generation Gas Separation Membranes. *J. Mater. Chem. A* **2014**, *2* (14), 4999−5009.
(35) Wright, R. A. E.; Wang, K.; Qu, J.; Zhao, B. Oil-Soluble Polymer Brush Grafted Nanoparticles as Effective Lubricant Additives for Friction and Wear Reduction. *Angew. Chem., Int. Ed.* **2016**, *55* (30), 8656−8660.
(36) Kim, D. J.; Kang, S. M.; Kong, B.; Kim, W.-J.; Paik, H.-j.; Choi, H.; Choi, I. S. Formation of Thermoresponsive Gold Nanoparticle/PNIPAAm Hybrids by Surface-Initiated, Atom Transfer Radical Polymerization in Aqueous Media. *Macromol. Chem. Phys.* **2005**, *206* (19), 1941−1946.
(37) Wei, Q.; Ji, J.; Shen, J. Synthesis of Near-Infrared Responsive Gold Nanorod/PNIPAAm Core/Shell Nanohybrids via Surface Initiated ATRP for Smart Drug Delivery. *Macromol. Rapid Commun.* **2008**, *29* (8), 645−650.
(38) Ma, H.; Hyun, J.; Stiller, P.; Chilkoti, A. Non-Fouling" Oligo (ethylene glycol)-Functionalized Polymer Brushes Synthesized by Surface-Initiated Atom Transfer Radical Polymerization. *Adv. Mater.* **2004**, *16* (4), 338−341.
(39) Hua, Z.; Yang, J.; Wang, T.; Liu, G.; Zhang, G. Transparent Surface with Reversibly Switchable Wettability between Superhydrophobicity and Superhydrophilicity. *Langmuir* **2013**, *29* (33), 10307−10312.

DOI: 10.1021/acs.macromol.7b00280
Macromolecules 2017, 50, 4151−4159

(40) Yang, Q.; Tian, J.; Hu, M.-X.; Xu, Z.-K. Construction of a Comb-like Glycosylated Membrane Surface by a Combination of UV-Induced Graft Polymerization and Surface-Initiated ATRP. *Langmuir* **2007**, *23* (12), 6684−6690.
(41) Frost, S.; Ulbricht, M. Thermoresponsive Ultrafiltration Membranes for the Switchable Permeation and Fractionation of Nanoparticles. *J. Membr. Sci.* **2013**, *448*, 1−11.
(42) Zhi, S.-H.; Xu, J.; Deng, R.; Wan, L.-S.; Xu, Z.-K. Poly(vinylidene fluoride) Ultrafiltration Membranes Containing Hybrid Silica Nanoparticles: Preparation, Characterization and Performance. *Polymer* **2014**, *55* (6), 1333−1340.
(43) He, K.; Duan, H.; Chen, G. Y.; Liu, X.; Yang, W.; Wang, D. Cleaning of Oil Fouling with Water Enabled by Zwitterionic Polyelectrolyte Coatings: Overcoming the Imperative Challenge of Oil−Water Separation Membranes. *ACS Nano* **2015**, *9* (9), 9188−9198.
(44) Matyjaszewski, K. Atom Transfer Radical Polymerization (ATRP): Current Status and Future Perspectives. *Macromolecules* **2012**, *45* (10), 4015−4039.
(45) Matyjaszewski, K.; Tsarevsky, N. V. Macromolecular Engineering by Atom Transfer Radical Polymerization. *J. Am. Chem. Soc.* **2014**, *136* (18), 6513−6533.
(46) Jakubowski, W.; Matyjaszewski, K. Activators Regenerated by Electron Transfer for Atom-Transfer Radical Polymerization of (Meth)acrylates and Related Block Copolymers. *Angew. Chem.* **2006**, *118* (27), 4594−4598.
(47) Jakubowski, W.; Min, K.; Matyjaszewski, K. Activators Regenerated by Electron Transfer for Atom Transfer Radical Polymerization of Styrene. *Macromolecules* **2006**, *39* (1), 39−45.
(48) Simakova, A.; Averick, S. E.; Konkolewicz, D.; Matyjaszewski, K. Aqueous ARGET ATRP. *Macromolecules* **2012**, *45* (16), 6371−6379.
(49) Matyjaszewski, K.; Coca, S.; Gaynor, S. G.; Wei, M.; Woodworth, B. E. Zerovalent Metals in Controlled/"Living" Radical Polymerization. *Macromolecules* **1997**, *30* (23), 7348−7350.
(50) Konkolewicz, D.; Wang, Y.; Zhong, M.; Krys, P.; Isse, A. A.; Gennaro, A.; Matyjaszewski, K. Reversible-Deactivation Radical Polymerization in the Presence of Metallic Copper. A Critical Assessment of the SARA ATRP and SET-LRP Mechanisms. *Macromolecules* **2013**, *46* (22), 8749−8772.
(51) Konkolewicz, D.; Wang, Y.; Krys, P.; Zhong, M.; Isse, A. A.; Gennaro, A.; Matyjaszewski, K. SARA ATRP or SET-LRP. End of Controversy? *Polym. Chem.* **2014**, *5* (15), 4396−4409.
(52) Matyjaszewski, K.; Jakubowski, W.; Min, K.; Tang, W.; Huang, J.; Braunecker, W. A.; Tsarevsky, N. V. Diminishing Catalyst Concentration in Atom Transfer Radical Polymerization with Reducing Agents. *Proc. Natl. Acad. Sci. U. S. A.* **2006**, *103* (42), 15309−15314.
(53) Konkolewicz, D.; Magenau, A. J. D.; Averick, S. E.; Simakova, A.; He, H.; Matyjaszewski, K. ICAR ATRP with ppm Cu Catalyst in Water. *Macromolecules* **2012**, *45* (11), 4461−4468.
(54) Ribelli, T. G.; Konkolewicz, D.; Bernhard, S.; Matyjaszewski, K. How are Radicals (Re)Generated in Photochemical ATRP? *J. Am. Chem. Soc.* **2014**, *136* (38), 13303−13312.
(55) Pan, X.; Tasdelen, M. A.; Laun, J.; Junkers, T.; Yagci, Y.; Matyjaszewski, K. Photomediated Controlled Radical Polymerization. *Prog. Polym. Sci.* **2016**, *62*, 73−125.
(56) Magenau, A. J. D.; Strandwitz, N. C.; Gennaro, A.; Matyjaszewski, K. Electrochemically Mediated Atom Transfer Radical Polymerization. *Science* **2011**, *332* (6025), 81−84.
(57) Park, S.; Chmielarz, P.; Gennaro, A.; Matyjaszewski, K. Electrochemically Mediated Atom Transfer Radical Polymerization Using a Sacrificial Anode. *Angew. Chem., Int. Ed.* **2015**, *54* (8), 2388−2392.
(58) Chmielarz, P.; Fantin, M.; Park, S.; Isse, A. A.; Gennaro, A.; Magenau, A. J. D.; Sobkowiak, A.; Matyjaszewski, K. Electrochemically Mediated Atom Transfer Radical Polymerization (*e*ATRP). *Prog. Polym. Sci.* **2017**, *69*, 47−78.
(59) Treat, N. J.; Sprafke, H.; Kramer, J. W.; Clark, P. G.; Barton, B. E.; Read de Alaniz, J.; Fors, B. P.; Hawker, C. J. Metal-Free Atom Transfer Radical Polymerization. *J. Am. Chem. Soc.* **2014**, *136* (45), 16096−16101.
(60) Pan, X.; Lamson, M.; Yan, J.; Matyjaszewski, K. Photoinduced Metal-Free Atom Transfer Radical Polymerization of Acrylonitrile. *ACS Macro Lett.* **2015**, *4* (2), 192−196.
(61) Zou, Y.; Kizhakkedathu, J. N.; Brooks, D. E. Surface Modification of Polyvinyl Chloride Sheets via Growth of Hydrophilic Polymer Brushes. *Macromolecules* **2009**, *42* (9), 3258−3268.
(62) Li, B.; Yu, B.; Huck, W. T. S.; Zhou, F.; Liu, W. Electrochemically Induced Surface-Initiated Atom-Transfer Radical Polymerization. *Angew. Chem., Int. Ed.* **2012**, *51* (21), 5092−5095.
(63) Yan, J.; Li, B.; Zhou, F.; Liu, W. Ultraviolet Light-Induced Surface-Initiated Atom-Transfer Radical Polymerization. *ACS Macro Lett.* **2013**, *2* (7), 592−596.
(64) Yan, J.; Pan, X.; Schmitt, M.; Wang, Z.; Bockstaller, M. R.; Matyjaszewski, K. Enhancing Initiation Efficiency in Metal-Free Surface-Initiated Atom Transfer Radical Polymerization (SI-ATRP). *ACS Macro Lett.* **2016**, *5*, 661−665.
(65) Song, Y.; Ye, G.; Lu, Y.; Chen, J.; Wang, J.; Matyjaszewski, K. Surface-Initiated ARGET ATRP of Poly(glycidyl methacrylate) from Carbon Nanotubes via Bioinspired Catechol Chemistry for Efficient Adsorption of Uranium Ions. *ACS Macro Lett.* **2016**, *5* (3), 382−386.
(66) Discekici, E. H.; Pester, C. W.; Treat, N. J.; Lawrence, J.; Mattson, K. M.; Narupai, B.; Toumayan, E. P.; Luo, Y.; McGrath, A. J.; Clark, P. G.; Read de Alaniz, J.; Hawker, C. J. Simple Benchtop Approach to Polymer Brush Nanostructures Using Visible-Light-Mediated Metal-Free Atom Transfer Radical Polymerization. *ACS Macro Lett.* **2016**, *5* (2), 258−262.
(67) Chmielarz, P.; Krys, P.; Wang, Z.; Wang, Y.; Matyjaszewski, K. Well-Defined Polymer Brushes from Silicon Wafers via Surface-Initiated *se*ATRP. *Macromol. Chem. Phys.* **2017**, DOI: 10.1002/macp.201700106.
(68) Fantin, M.; Isse, A. A.; Venzo, A.; Gennaro, A.; Matyjaszewski, K. Atom Transfer Radical Polymerization of Methacrylic Acid: A Won Challenge. *J. Am. Chem. Soc.* **2016**, *138* (23), 7216−7219.
(69) Chmielarz, P.; Sobkowiak, A.; Matyjaszewski, K. A Simplified Electrochemically Mediated ATRP Synthesis of PEO-*b*-PMMA Copolymers. *Polymer* **2015**, *77*, 266−271.
(70) Chmielarz, P.; Park, S.; Sobkowiak, A.; Matyjaszewski, K. Synthesis of β-Cyclodextrin-Based Star Polymers via a Simplified Electrochemically Mediated. *Polymer* **2016**, *88*, 36−42.
(71) Chmielarz, P. Cationic Star Polymers by Simplified Electrochemically Mediated ATRP. *eXPRESS Polym. Lett.* **2016**, *10* (10), 810−821.
(72) Chmielarz, P. Synthesis of α-D-Glucose-Based Star Polymers through Simplified Electrochemically Mediated ATRP. *Polymer* **2016**, *102*, 192−198.
(73) Lorandi, F.; Fantin, M.; Isse, A. A.; Gennaro, A. Electrochemically Mediated Atom Transfer Radical Polymerization of *n*-Butyl Acrylate on Non-Platinum Cathodes. *Polym. Chem.* **2016**, *7* (34), 5357−5365.
(74) Chmielarz, P. Cellulose-Based Graft Copolymers Prepared by Simplified Electrochemically Mediated ATRP. *eXPRESS Polym. Lett.* **2017**, *11* (2), 140−151.
(75) Chmielarz, P. Synthesis of Multiarm Star Block Copolymers via Simplified Electrochemically Mediated ATRP. *Chemical Papers* **2017**, *71* (1), 161−170.
(76) Yan, J.; Pan, X.; Wang, Z.; Zhang, J.; Matyjaszewski, K. Influence of Spacers in Tetherable Initiators on Surface-Initiated Atom Transfer Radical Polymerization (SI-ATRP). *Macromolecules* **2016**, *49* (23), 9283−9286.
(77) Choi, J.; Dong, H.; Matyjaszewski, K.; Bockstaller, M. R. Flexible Particle Array Structures by Controlling Polymer Graft Architecture. *J. Am. Chem. Soc.* **2010**, *132* (36), 12537−12539.
(78) Munirasu, S.; Karunakaran, R. G.; Rühe, J. r.; Dhamodharan, R. Synthesis and Morphological Study of Thick Benzyl Methacrylate−Styrene Diblock Copolymer Brushes. *Langmuir* **2011**, *27* (21), 13284−13292.

DOI: 10.1021/acs.macromol.7b00280
Macromolecules 2017, 50, 4151−4159

(79) Ohno, K.; Tabata, H.; Tsujii, Y. Surface-Initiated Living Radical Polymerization from Silica Particles Functionalized with Poly(ethylene glycol)-Carrying Initiator. *Colloid Polym. Sci.* **2013**, *291* (1), 127−135.
(80) Hui, C. M.; Dang, A.; Chen, B.; Yan, J.; Konkolewicz, D.; He, H.; Ferebee, R.; Bockstaller, M. R.; Matyjaszewski, K. Effect of Thermal Self-Initiation on the Synthesis, Composition, and Properties of Particle Brush Materials. *Macromolecules* **2014**, *47* (16), 5501−5508.
(81) Konkolewicz, D.; Krys, P.; Góis, J. R.; Mendonça, P. V.; Zhong, M.; Wang, Y.; Gennaro, A.; Isse, A. A.; Fantin, M.; Matyjaszewski, K. Aqueous RDRP in the Presence of Cu^0: The Exceptional Activity of Cu^I Confirms the SARA ATRP Mechanism. *Macromolecules* **2014**, *47* (2), 560−570.
(82) Magenau, A. J. D.; Bortolamei, N.; Frick, E.; Park, S.; Gennaro, A.; Matyjaszewski, K. Investigation of Electrochemically Mediated Atom Transfer Radical Polymerization. *Macromolecules* **2013**, *46* (11), 4346−4353.
(83) Krys, P.; Ribelli, T. G.; Matyjaszewski, K.; Gennaro, A. Relation between Overall Rate of ATRP and Rates of Activation of Dormant Species. *Macromolecules* **2016**, *49* (7), 2467−2476.
(84) Krys, P.; Matyjaszewski, K. Kinetics of Atom Transfer Radical Polymerization. *Eur. Polym. J.* **2017**, *89*, 482−523.
(85) Konkolewicz, D.; Schröder, K.; Buback, J.; Bernhard, S.; Matyjaszewski, K. Visible Light and Sunlight Photoinduced ATRP with ppm of Cu Catalyst. *ACS Macro Lett.* **2012**, *1* (10), 1219−1223.
(86) Goel, V.; Pietrasik, J.; Dong, H.; Sharma, J.; Matyjaszewski, K.; Krishnamoorti, R. Structure of Polymer Tethered Highly Grafted Nanoparticles. *Macromolecules* **2011**, *44* (20), 8129−8135.
(87) Daoud, M.; Cotton, J. P. Star Shaped Polymers: A Model for the Conformation and its Concentration Dependence. *J. Phys. (Paris)* **1982**, *43* (3), 531−538.
(88) Sakar, D.; Erdogan, T.; Cankurtaran, O.; Hizal, G.; Karaman, F.; Tunca, U. Physicochemical Characterization of Poly(*tert*-butyl acrylate-*b*-methyl methacrylate) Prepared with Atom Transfer Radical Polymerization by Inverse Gas Chromatography. *Polymer* **2006**, *47* (1), 132−139.
(89) Danial, M.; My-Nhi Tran, C.; Young, P. G.; Perrier, S.; Jolliffe, K. A. Janus Cyclic Peptide−Polymer Nanotubes. *Nat. Commun.* **2013**, *4*, 2780.
(90) Lewin, M.; Mey-Marom, A.; Frank, R. Surface Free Energies of Polymeric Materials, Additives and Minerals. *Polym. Adv. Technol.* **2005**, *16* (6), 429−441.
(91) Schmitt, M.; Hui, C. M.; Urbach, Z.; Yan, J.; Matyjaszewski, K.; Bockstaller, M. R. TailoringStructure Formation and Mechanical Properties of Particle Brush Solids via Homopolymer Addition. *Faraday Discuss.* **2016**, *186* (0), 17−30.

DOI: 10.1021/acs.macromol.7b00280
Macromolecules 2017, 50, 4151−4159